JOURNAL OF CATALYSIS 95, 193–201 (1985)

Supported Liquid-Phase Catalysis

II. Experimental Evaluation of the Flux Model for Liquid-Loaded Porous Media

RAVINDRA DATTA,* WILLIAM SAVAGE,†,[1] AND ROBERT G. RINKER†

*Chemical and Materials Engineering Department, University of Iowa, Iowa City, Iowa 52242, and †Department of Chemical and Nuclear Engineering, University of California, Santa Barbara, California 93106

Received October 16, 1984; revised April 11, 1985

An experimental investigation was undertaken to test the model for transport of gases in liquid-impregnated porous media proposed in Part I (R. Datta and R. G. Rinker, *J. Catal.* **95,** 181, 1985) of this series. It was found that the original dusty-gas model needs to be modified by incorporating an additional slip-flow correction factor, σ, in order to reconcile differences in the values of the Knudsen diffusion constant, C_1^0, obtained separately from isobaric diffusion and flow experiments. Based on the results of the permeability experiments with pure gases and binary mixtures and earlier isobaric diffusion experiments, it is concluded that the correlations proposed to account for the variation of the dusty-gas parameters C_0^G, C_1^G, and C_2^G with degree of liquid loading are entirely adequate. It is also indicated that the dispersion pattern of liquids with a contact angle less than 90° is substantially the same in a given porous medium.

1. INTRODUCTION

In Part I of this series (*1*), a model was developed for the transport and chemical reaction of gaseous species in supported liquid-phase catalysis (SLPC) in which a catalytic liquid is dispersed within an inert porous support. This part is concerned with the experimental verification of the flux model without reaction by studying the transport of gases in porous media supporting varying amounts of noncatalytic liquid. The testing of the complete transport and reaction model is considered in Part III.

The model for SLPC proposed in Part I is based primarily on the assumption that the dusty-gas model (*2*) is applicable for the flux in residual gas pore space of a liquid-loaded porous medium. The dusty-gas model was chosen because it is one of the more comprehensive and useful flux models currently available. Nevertheless, it is known to have certain shortcomings and some comments are in order in this regard.

As originally conceived, the dusty-gas model is understood to be applicable to unimodal, macroporous, isotropic porous media. The three dusty-gas parameters, C_0, C_1, and C_2, introduced in its formulation, are regarded as adjustable parameters to be estimated from flux measurements. For this purpose, at least two sets of experiments are required (*3*), namely, isobaric diffusion measurements and permeability measurements under the influence of a pressure gradient. The isobaric binary diffusion measurements over a wide range of operating pressures can be used to evaluate C_1 and C_2. Subsequent permeability experiments yield C_0 and C_1 again. These two sets of experiments, therefore, also serve as a check on the adequacy of the dusty-gas model for the given porous medium. Thus, the values of C_1 evaluated separately from diffusion and permeability measurements on a macroporous fritted glass filter were found (*4, 5*) to be equal within experimental error, and it was concluded that the dusty-gas model was indeed applicable. However, other investigators have found

[1] Current address: General Dynamics Corporation, Convair Division, San Diego, Calif. 92111.

0021-9517/85 $3.00

the original dusty-gas model to be inadequate for commercial bimodal porous pellets and also for unimodal microporous pellets (*6–8*). Thus, it was found necessary (*6*) to introduce an additional constant, σ, in order to reconcile the differences in values of C_1 obtained individually from diffusion and permeability experiments. The constant σ, a slip-flow correction factor, was defined as simply the ratio of C_1 evaluated from permeability experiments to that evaluated from isobaric diffusion experiments. With this additional constant, the extended dusty-gas model was found to be successful in accurately predicting the fluxes under the combined influence of composition and pressure gradients.

In a somewhat different approach (*8*) volume-mean diffusion and slip-flow correction factors were introduced to account for the deviations attributed to the heteroporosity effects in porous materials with wide pore-size distributions. The pore-size distribution was used to estimate these correction factors and succeeded in obtaining substantially improved predictions.

Mindful of the possible inadequacy of the original dusty-gas model for flux in liquid-loaded porous media, we elected to adopt the first modified form of the dusty-gas model discussed above (*6*) for the present study. This approach was chosen because of its relative simplicity and because it requires a single extra parameter, σ, which can be estimated without additional experimentation. Since the emphasis here is rather on studying the effect of liquid loading, the question of modification of the general dusty-gas equation by introducing a viscous-slip term will be addressed in a separate publication.

2. THEORY

For a binary gas mixture of A and B, the dusty-gas model (Eq. (2), Part I) flux equations can be solved simultaneously to yield explicit expressions for the individual fluxes N_A^G and N_B^G (*3*). Adding the liquid-phase fluxes (Eq. (26), Part I) to these, incorporating the slip-flow correction factor, σ, and using Eqs. (3) and (4) of Part I, the resulting expression for the one-dimensional overall flux of A in liquid-loaded porous media is

$$N_A = -\frac{P}{R_g T}\left\{\frac{C_2^G C_1^G D_{AB}^O v_A}{C_2^G D_{AB}^O + PC_1^G(x_A v_B + x_B v_A)} + C_2^L D_A^L H_A\right\}\frac{dx_A}{dz} - \frac{x_A}{R_g T}\left\{\frac{\sigma C_1^G v_A (C_2^G D_{AB}^O + PC_1^G v_B)}{C_2^G D_{AB}^O + PC_1^G(x_A v_B + x_B v_A)} + \frac{C_0^G P}{\mu_m} + C_2^L D_A^L H_A\right\}\frac{dP}{dz}, \quad (1)$$

where

$$D_{AB}^O = D_{AB}P \quad (2)$$

and is independent of pressure.

A similar expression can also be written for the flux of B simply by interchanging the suffixes A and B in Eq. (1). It may also be noted that for $\sigma = 1$, Eq. (1) reduces to the corresponding expression obtained from the original dusty-gas model.

(*a*) *Isobaric Binary Diffusion*

For isobaric diffusion of a binary gas mixture, setting $dP/dz = 0$ and rearranging

$$N_A = -\frac{P}{R_g T}\left\{\frac{1}{1/C_1^G v_A + (1 - \alpha x_A)/C_2^G D_{AB}} + C_2^L D_A^L H_A\right\}\frac{dx_A}{dz}, \quad (3)$$

where

$$\alpha = 1 - v_B/v_A = 1 - (M_A/M_B)^{1/2}. \quad (4)$$

For binary counter-diffusion across a porous pellet of thickness L, the boundary conditions for Eq. (3) are

$$\text{at } z = 0, \quad x_A = x_{A0} \quad (5)$$

$$\text{at } z = L, \quad x_A = x_{AL}. \quad (6)$$

Integrating Eq. (3) subject to these boundary conditions

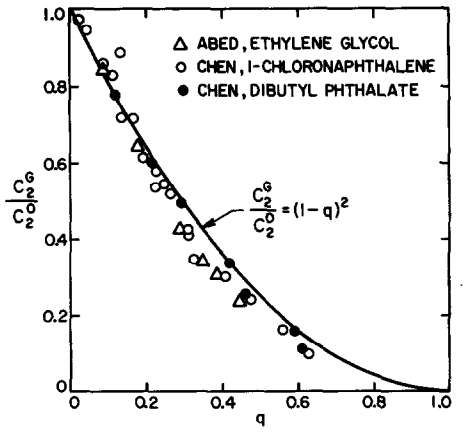

FIG. 1. C_2^G/C_2^0 versus the liquid-loading q. Comparison of Eq. (24), Part I, with experimental results of others (*9, 10*) for isobaric counter-diffusion of helium and nitrogen through liquid-loaded T-708 pellets.

$$N_A = \frac{PC_2^G D_{AB}}{R_g T L \alpha} \ln \left\{ \frac{1 - \alpha x_{AL} + C_2^G D_{AB}/C_1^G v_A}{1 - \alpha x_{A0} + C_2^G D_{AB}/C_1^G v_A} \right\} + \frac{PC_2^L D_A^L H_A}{R_g T} (x_{A0} - x_{AL}). \quad (7)$$

It is most convenient to estimate C_2^G by performing experiments with sparingly soluble gases ($H_A \to 0$) and under high pressure so that molecular diffusion dominates. Under these conditions, Eq. (7) simplifies to

$$N_A = \frac{PC_2^G D_{AB}}{R_g T L \alpha} \ln \left\{ \frac{1 - \alpha x_{AL}}{1 - \alpha x_{A0}} \right\}. \quad (8)$$

Thus C_2^G can be estimated directly from flux measurements. Such experiments were performed (*9, 10*) involving isobaric binary counter-diffusion of helium and nitrogen using a modified version of the Wicke–Kallenbach diffusion cell. The porous support used in that work consisted of Girdler T-708 α-alumina pellets. These pellets are fairly macroporous, and thus, experiments mostly at pressures above 2 MPa ensured that the flux was predominately by molecular diffusion in the residual gas pore space. The pellets were loaded to varying extents with three different liquids, namely, ethylene glycol, 1-chloronaphthalene, and dibutyl phthalate. The values of the ratio C_2^G/C_2^0 obtained are plotted against the liquid-loading q in Fig. 1 and are also compared against Eq. (24) of Part I. It can be seen that the agreement is good, especially for $q < 0.3$. At higher liquid loadings, however, some deviation is observed. Equation (24) of Part I was first proposed (*9*) as an empirical expression that best described the experimental results with ethylene glycol. The other significant conclusion that can be gleaned from these results is that, in all likelihood, the dispersion pattern of liquids with contact angles <90° is essentially the same in a given porous support. It may be noted that the other properties (polarity, viscosity, etc.) of the three liquids employed are quite different.

(*b*) *Flow of a Pure Gas*

For the flow of a pure gas in a liquid-loaded pellet induced by a pressure gradient, Eq. (1) reduces to

$$N_A = -\frac{1}{R_g T} \left(\sigma C_1^G v_A + \frac{C_0^G P}{\mu_A} + C_2^L D_A^L H_A \right) \frac{dP}{dz} \quad (9)$$

subject to the boundary conditions

$$\text{at } z = 0, \quad P = P_0 \quad (10)$$

$$\text{at } z = L, \quad P = P_L. \quad (11)$$

Under these conditions, integration of Eq. (9) and rearrangement produces the dimensionless working form

$$\frac{N_A R_g T}{v_A \Delta P} = \frac{\sigma C_1^G}{L} + \frac{C_2^L D_A^L H_A}{v_A L} + \frac{C_0^G}{L^2} \left(\frac{\bar{P} L}{\mu_A v_A} \right), \quad (12)$$

where

$$\Delta P = P_0 - P_L \quad (13)$$

and

$$\bar{P} = \frac{P_0 + P_L}{2}. \quad (14)$$

If the left-hand side of Eq. (12) is plotted against the term in the parentheses on the right-hand side for a variety of mean pressures $\bar{P}$, the points should lie on a straight line with a slope of C_0^G/L^2 and an intercept equal to the sum of the first two terms on the right-hand side. Further, the second term would often be negligible compared to the first, unless A is highly soluble in the liquid. Thus, for sparingly soluble gases, C_0^G and the product σC_1^G can be evaluated directly. If C_1^G were independently evaluated from low-pressure isobaric diffusion experiments (Eq. (7)), then the slip-flow correction factor σ can also be determined.

(c) Flow of a Binary Gas Mixture

Flow experiments may also be performed with gas mixtures. When only pressure gradients are present, substituting $dx_A/dz = 0$ in Eq. (1), and $dx_B/dz = 0$ in the analogous expression for B, and adding the resulting expressions to obtain the total flux, $N_T = N_A + N_B$,

$$N_T = -\frac{1}{R_g T}\left[\frac{\sigma\{C_2^G D_{AB}^O(1-\alpha x_B) + PC_1^G v_B\}}{C_2^G D_{AB}^O/C_1^G v_A + P(1-\alpha x_A)} + \frac{C_0^G P}{\mu_m} + C_2^L(x_A D_A^L H_A + x_B D_B^L H_B)\right]\frac{dP}{dz}. \quad (15)$$

For constant composition, Eq. (15) can be integrated subject to the boundary conditions of Eqs. (10) and (11) and rearranged into the form

$$\frac{N_T R_g T(1-\alpha x_A)}{v_B} = \left[\frac{\sigma C_1^G}{L} + \frac{C_0^G}{L^2}\left\{\frac{\bar{P}L(1-\alpha x_A)}{\mu_m v_B}\right\} + C_2^L(x_A D_A^L H_A + x_B D_B^L H_B)\frac{(1-\alpha x_A)}{v_B L}\right]\Delta P + \frac{\sigma C_2^G D_{AB}^O}{L v_B}[1-\alpha x_B-(1-\alpha)/(1-\alpha x_A)]\ln\left\{\frac{\frac{C_2^G D_{AB}^O}{C_1^G v_A}+(1-\alpha x_A)P_0}{\frac{C_2^G D_{AB}^O}{C_1^G v_A}+(1-\alpha x_A)P_L}\right\}. \quad (16)$$

It may be noted that Eq. (16) reduces to Eq. (12) for the flow of a pure gas by substituting $x_A = 1$. For sufficiently small pressure drops such that $P_0 \approx P_L$, the last term on the right-hand side of Eq. (16) becomes small compared to the first term. Additionally, when gases A and B are not highly soluble, Eq. (16) simplifies to

$$\frac{N_T R_g T(1-\alpha x_A)}{v_B} = \left[\frac{\sigma C_1^G}{L} + \frac{C_0^G}{L^2}\left\{\frac{\bar{P}L(1-\alpha x_A)}{\mu_m v_B}\right\}\right]\Delta P. \quad (17)$$

This equation may be used in two different ways. Dividing throughout by ΔP, it takes on the dimensionless form of Eq. (12), and hence may be plotted in a similar manner. Then σC_1^G and C_0^G can be determined from the intercept and the slope, respectively, as before. Alternatively, the left-hand side of Eq. (17) may be plotted against ΔP, for a constant mean pressure $\bar{P}$, to give a straight line passing through the origin. If experiments are performed at two different mean pressures, $\bar{P}_1$ and $\bar{P}_2$, for varying ΔP, two straight lines with different slopes are obtained. Then the two unknowns σC_1^G and C_0^G can be found by simultaneous solution of the two resulting equations. In our experiments we followed the former approach for flow of pure gases and the latter approach for binary gas mixtures for reasons of experimental convenience.

3. APPARATUS AND PROCEDURE

Permeability experiments with pure gases and binary mixtures in liquid-loaded porous media were conducted at room temperature in the modified Wicke–Kallenbach diffusion cell constructed earlier (*11*). A detailed description of the apparatus is given elsewhere (*6*). The cell is designed to operate at relatively high pressures of up to 7 MPa, each compartment containing magnetic stirrers.

The porous support used in this study is T-708, α-alumina, in the form of 6.4×10^{-3} by 6.4×10^{-3} m cylindrical pellets, supplied by Girdler Catalysts Division of Chemetron

Corporation. This support was also used by previous investigators (*9, 10*) for isobaric diffusion experiments in liquid-loaded pellets. These pellets are predominantly macroporous. Pore-size distribution data and other physical characteristics of T-708 pellets are given elsewhere (*12*). The liquid selected for loading in the porous support is tetralin (1,2,3,4-tetrahydronaphthalene) which is a nonpolar solvent with low viscosity and has a contact angle of less than 90°. In addition, it has low volatility (its vapor pressure is 26 Pa at 293 K) and is, therefore, an appropriate solvent for potential use in SLPC. Nitrogen and argon were used in experiments involving permeability of pure gases as well as binary mixtures. In addition, experiments were performed with binary mixtures of cyclopentane vapor and either nitrogen or argon. Cyclopentane was chosen because of its moderate solubility in tetralin in order to study the effect of gas solubility on its transport in liquid-loaded porous media.

Experiments were performed using eight cylindrical pellets mounted snugly in holes drilled in a Teflon disk of the same thickness as the pellets in order to seal off the cylindrical sides and expose only the flat faces. This disk was then placed between the two compartments of the diffusion cell and sealed off to ensure transport of gases from one compartment to the other only through the pellets.

The procedure used to impregnate the pellets with tetralin was as follows: The eight pellets to be used in a given run were placed under vacuum for a minimum of 72×10^3 s. Tetralin was then mixed with chloroform in a volumetric ratio corresponding to the desired degree of liquid loading. While the system remained evacuated, enough solution was added to immerse the pellets completely. The pellets were exposed to the solution for a period of 5×10^5 to 6×10^5 s, enabling it to penetrate completely. It was verified that the solution penetrates the pellet completely by dissolving a dye, 1,1-diphenyl-2-picrylhydrazyl (DPPH) in the tetralin–chloroform mixture and later breaking open a loaded pellet. After being removed from solution, the pellets were placed under vacuum for 3.6×10^3 s in a clean flask to remove the bulk of the chloroform; the latter has a vapor pressure roughly 500 times that of tetralin. Evaporation of the chloroform carrier leaves the tetralin dispersed on the pore walls.

Since cyclopentane is a liquid at room temperature (boiling point = 322.3 K), in experiments involving cyclopentane a sparging apparatus was used to introduce its vapors into the diffusion cell. Thus, a carrier gas (nitrogen or argon) is introduced through a sparger constructed from a porous stainless-steel tube made of laminated wire mesh bonded together with effective hole diameters on the order of 100 μm. The gas bubbles through the liquid become saturated with its vapor. The temperature of the sparging unit is kept below room temperature (at 288 K) using a constant-temperature bath equipped with a refrigeration unit. This is done to prevent the vapors from condensing in the tubing. Two filters are also positioned after the sparging unit to eliminate the possibility of any aerosol being transported.

In a typical run, the cell is loaded with eight pellets, reassembled, and carefully tested for any leaks. The permeating gas or gas mixture is then simultaneously introduced into both the compartments and the pressure gradually raised to the desired operating pressure while the differential pressure gauge is monitored so as to avoid excessive pressure drops across the pellets. The flow is adjusted using needle valves. Finally, certain valves are closed to permit the feed to be introduced only to one compartment of the cell and to exit through the opposite cell compartment. The system is allowed to reach steady state. Analysis of the inlet and effluent gas streams is performed using a Loenco Model 160 gas chromatograph with a thermal conductivity detector and an HP-3380 integrator–recorder.

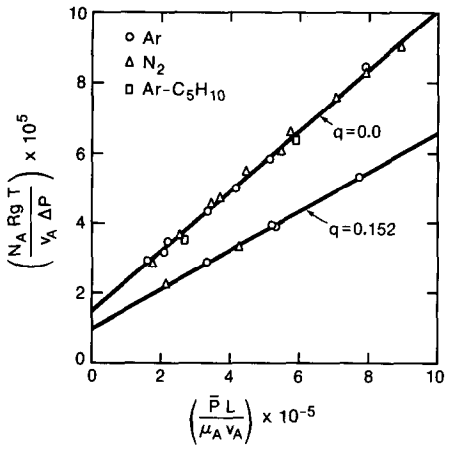

FIG. 2. Dimensionless specific flux versus the dimensionless mean pressure for permeability of a pure gas in T-708 pellets for $q = 0$ and $q = 15.2\%$. Also included are two data points for the argon–cyclopentane mixture.

4. RESULTS AND DISCUSSION

(a) *Flow of Pure Gas*

Equation (12) was used to analyze the experimental data obtained for permeability of two different gases, nitrogen and argon, in dry as well as liquid-loaded pellets. Figure 2 illustrates the results of plotting the dimensionless specific flux $N_A R_g T/v_A \Delta P$ versus the dimensionless pressure $\bar{P}L/\mu_A v_A$ for dry pellets ($q = 0$) and for a liquid loading of 15.2%, calculated from flow measurements at several different operating pressure ranging from about 0.25 to 1.3 MPa. All the data points for both gases from the experiments with dry pellets fall on the same straight line, whereas those for $q = 0.152$ can be correlated well by another straight line of a different slope and intercept. In a similar fashion, permeability data for higher liquid loadings were also correlated well. This clearly indicates that Eq. (12) is valid for both dry and liquid-loaded porous media. Further, the dusty-gas parameters are independent of the flowing gas but vary strongly with the liquid loading.

From the slope of the straight line obtained by linear regression on the data for dry pellets (correlation coefficient = 0.9983), $C_0^O = 2.99 \times 10^{-15}$ m^2, and from the intercept, $\sigma C_1^O = 870$ Å. Based on isobaric diffusion experiments, previous workers (*10*) recommend $C_1^O = 327$ Å for the T-708 pellets. Assuming this value for C_1^O, the slip-flow correction factor is $\sigma = 2.66$. In comparison, earlier studies (*6*) had given $\sigma = 2.3 \pm 0.3$ for these pellets. Similarly, for $q = 0.152$, from the slope of the straight line $C_0^G = 1.96 \times 10^{-15}$ m^2, and from the intercept $\sigma C_1^G = 585$ Å. Since the exact nature of the slip-flow correction factor is not fully known at present, it is assumed that σ is not a function of liquid loading. Then, for $q = 0.152$, $C_1^G = 222$ Å. For both nitrogen and argon, the second term on the right-hand side of Eq. (12) is negligible.

(b) *Flow of Binary Gas Mixture*

Equation (16) was used to analyze the data obtained from permeability experiments with three different binary mixtures, nitrogen–cyclopentane, argon–cyclopentane, and nitrogen–argon. Component A refers to cyclopentane in mixtures involving this component and to argon in nitrogen–argon mixtures. All the runs were conducted at two different mean pressures of approximately 0.3 and 0.8 MPa, and ΔP was varied in the range of 10×10^3 to 69×10^3 Pa.

Figure 3 illustrates a plot of $N_T R_g T(1 - \alpha x_A)/v_B$ against ΔP for the flow of a cyclo-

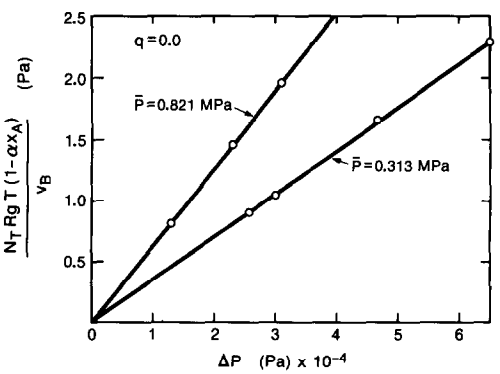

FIG. 3. Permeability of the argon–cyclopentane mixture in dry T-708 pellets at two different mean pressures.

pentane–argon mixture in a dry pellet at two different mean pressures. Similar plots were obtained for liquid-loaded pellets. Since the data are correlated very well (correlation coefficient = 0.9998) by two different straight lines passing through the origin, the magnitude of the last term on the right-hand side of Eq. (16) is evidently negligible under our experimental conditions. The slopes of these two straight lines obtained from linear regression provide two equations in the unknowns σC_1^O and C_0^O and are solved simultaneously to yield $C_0^O = 2.94 \times 10^{-15}$ m^2 and $\sigma C_1^O = 847$ Å. These values agree closely with those obtained from pure-gas permeability experiments, thus substantiating the validity of Eq. (16).

As mentioned before, these data could also be plotted in another manner. Thus, the average values of $N_T R_g T(1 - \alpha x_A)/v_B \Delta P$ are plotted against $\bar{P}L(1 - \alpha x_A)/\mu_m v_B$ in Fig. 2 for the two mean pressures shown in Fig. 3. These two data points fall close to the straight line obtained for the flow of pure gases, thus providing further proof of the adequacy of the relationships.

In the calculations for both pure-gas and mixture permeabilities, the viscosities of pure nitrogen and argon at the operating temperature and pressure were calculated from correlations (*13*). The viscosity of cyclopentane was calculated using a corresponding-states relationship (*14*). The viscosity of binary gas mixtures was estimated (*15*) by

$$\mu_m = \frac{x_A \mu_A}{x_A + x_B \phi_{AB}} + \frac{x_B \mu_B}{x_B + x_A \phi_{BA}}, \quad (18)$$

where

$$\phi_{AB} = \frac{[1 + (\mu_A/\mu_B)^{1/2}(M_B/M_A)^{1/4}]^2}{\{8[1 + (M_A/M_B)]\}^{1/2}} \quad (19)$$

and

$$\phi_{BA} = \phi_{AB} \frac{\mu_B}{\mu_A} \frac{M_A}{M_B}. \quad (20)$$

Several permeability runs were also made with binary gas mixtures flowing through pellets supporting varying amounts of liquid and were analyzed using Eq. (16). In runs involving cyclopentane, its mole fraction in the binary gas mixture varied approximately between 3.5% at $\bar{P} = 0.82$ MPa and 9% at $\bar{P} = 0.26$ MPa. The partition coefficients H_A of cyclopentane in tetralin at these pressures were estimated (*16*) to be approximately 23 and 11, respectively, using the Chao–Seader correlation (*17*). For these values, the liquid-phase contribution to the overall flux (third term within the square brackets on the right-hand side of Eq. (16)) was calculated to be negligible. Thus, as in the case of dry pellets, the slope of a straight line obtained by plotting the data in the manner of Fig. 3 was a function only of σC_1^G and C_0^G. These values could thus be calculated from the two straight lines obtained from experiments at two mean pressures for a given liquid loading. Linear regression in every case produced correlation coefficients better than 0.996.

Calculations were also made to consider the effect of the gas solubility on possible film swelling. It was estimated (*16*) that the effective liquid loading increases by approximately 2.5–3% due to the dissolution of cyclopentane in tetralin under the experimental conditions. This increase was incorporated in calculating the effective liquid loading for runs involving cyclopentane.

(c) *Variation of C_0^G and C_1^G with Liquid Loading*

The final values of σC_1^G and C_0^G calculated as described above for various liquid loadings are summarized in Table 1. For the dry pellets, the average values are $C_0^O = 2.97 \times 10^{-15}$ m^2, $C_0^O = 327$ Å, and $\sigma = 2.63$. These values are used in obtaining the ratios C_1^G/C_1^O and C_0^G/C_0^O which are plotted in Figs. 4 and 5 along with the corresponding theoretical expressions proposed in Part I. Generally, the agreement is very good. It is also noteworthy that nonlinear regression analyses of the data presented in Figs. 4 and 5 were performed (*16*), wherein the exponent n was left unspecified in the expres-

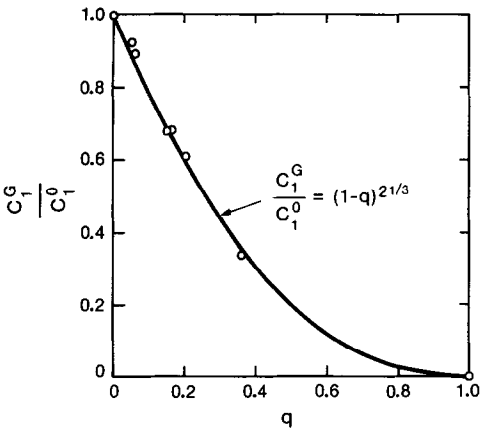

FIG. 4. C_1^G/C_1^O versus the liquid-loading q. Comparison of Eq. (23), Part I, with experimental results for tetralin-loaded T-708 pellets.

sions $C_1^G/C_1^O = (1 - q)^n$ and $C_0^G/C_0^O = (1 - q)^n$. The values of n obtained for the best fits were $n = 2.251 \pm 0.174$ for C_1^G/C_1^O and $n = 2.595 \pm 0.131$ for C_0^G/C_0^O. Clearly, these fitted values of n include the theoretical values of $2\frac{1}{3}$ and $2\frac{2}{3}$, respectively. The maximum relative deviation between the experimental and predicted values for C_1^G/C_1^O is 5.1% and that for C_0^G/C_0^O is 2.8%. Thus the proposed model agrees well with our experimental results for liquid-loaded T-708 pellets. Further experimentation is required to check the applicability of the model to other porous supports as well as to verify the contribution of the liquid phase to the flux of soluble gases.

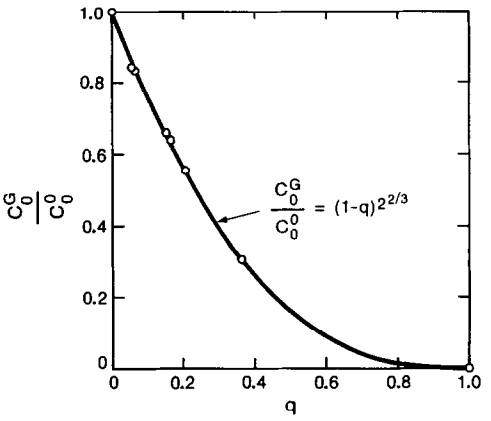

FIG. 5. C_0^G/C_0^O versus the liquid-loading q. Comparison of Eq. (22), Part I, with experimental results for tetralin-loaded T-708 pellets.

TABLE I

Results of Permeability Experiments with Liquid-Loaded T-708 Pellets

Liquid-loading q (%)	Loaded solvent	Flowing gas(es)	σC_1^G (Å)	$C_0^G \times 10^{15}$ (m^2)
0.0	Dry pellet	N_2; Ar	870	2.99
0.0	Dry pellet	Ar–C_5H_{10}	847	2.94
5.6	T	N_2–Ar	793	2.50
6.2	T + C_5H_{10}	N_2–C_5H_{10}	765	2.48
15.2	T	N_2; Ar	585	1.96
16.3	T + C_5H_{10}	N_2–C_5H_{10}	587	1.90
20.5	T + C_5H_{10}	N_2–C_5H_{10}	523	1.65
36.1	T + C_5H_{10}	N_2–C_5H_{10}	289	0.908

Note. T = tetralin; C_5H_{10} = cyclopentane.

5. CONCLUSION

Permeability experiments were performed involving flow of pure gases and binary mixtures in T-708 pellets supporting varying amounts of tetralin. The results from these experiments, in addition to those obtained by others (*9, 10*) for isobaric binary counter-diffusion experiments with these pellets, led to the conclusion that the extended form of the dusty-gas model, incorporating an additional slip-flow correction constant (*6*), can be successfully applied to gas-phase transport in liquid-loaded porous media. In addition, it is shown that the variation of the dusty-gas parameters C_0^G, C_1^G, and C_2^G for the residual gas pore space with liquid loading can be adequately predicted by the proposed Eqs. (22), (23), and (24), respectively, in Part I. Another significant conclusion based on experimental results with four different liquids is that the dispersion pattern of liquids with contact angles less than 90° is essentially the same in a given porous medium.

Additional experimentation is needed to (a) check the contribution of the liquid phase to the overall flux of soluble gases, (b) check the adequacy of the transport model for other porous supports, and (c) extend the model to include nonwetting liquids, i.e., those with contact angles >90°.

APPENDIX: NOMENCLATURE

Refer to the appendix of Part I. Additional symbols introduced in Part II are listed below.

D^{0}_{AB}	pressure-independent term defined as $D_{AB}P$ (m^2 Pa/s)
α	defined by $1 - (M_A/M_B)^{1/2}$ (dimensionless)
L	pellet thickness (m)
N_T	total molar flux = $N_A + N_B$ (mol/m^2 s)
$\bar{P}$	mean operating pressure = $(P_0 + P_L)/2$ (Pa)
P_L	pressure at pellet exit, $z = L$ (Pa)
P_0	pressure at pellet entrance, $z = 0$ (Pa)
ΔP	pressure difference across the pellet = $P_0 - P_L$ (Pa)
x_{AL}	mole fraction of A in the gas phase at $z = L$
x_{A0}	mole fraction of A in the gas phase at $z = 0$

Greek symbols

ϕ_{AB}, ϕ_{BA}	binary mixture viscosity parameters, Eqs. (19) and (20)
σ	slip-flow correction factor
μ_A, μ_B	viscosity of A and B, respectively (Pa · s)

ACKNOWLEDGMENT

This work was supported in part by the Division of Chemical Sciences (Office of Basic Energy Sciences) of the Department of Energy under Award DE-AM03-76SF00034 P.A. No. 234.

REFERENCES

1. Datta, R., and Rinker, R. G., *J. Catal.* **95,** 181 (1985).
2. Mason, E. A., Malinauskas, A. P., and Evans, R. B., III, *J. Chem. Phys.* **46,** 3199 (1967).
3. Jackson, R., "Transport in Porous Catalysts." Elsevier, New York, 1977.
4. Gunn, R. D., Ph.D. thesis. University of California, Berkeley, 1967.
5. Gunn, R. D., and King, C. J., *AIChE J.* **15,** 507 (1969).
6. Abed, R., and Rinker, R. G., *J. Catal.* **34,** 246 (1974).
7. Omata, H., and Brown, L. F., *AIChE J.* **18,** 967 (1972).
8. Chen, O. T., and Rinker, R. G., *Chem. Eng. Sci.* **34,** 51 (1979).
9. Abed, R., and Rinker, R. G., *J. Catal.* **31,** 119 (1973).
10. Chen, O. T., and Rinker, R. G., *Chem. Eng. Sci.* **33,** 1201 (1978).
11. Abed, R., Ph.D. thesis. University of California, Santa Barbara, 1973.
12. Chen, O. T., Ph.D. thesis. University of California, Santa Barbara, 1976.
13. Kestin, J., and Leidenfrost, W., *Physica* **25,** 1033 (1959).
14. Yoon, P., and Thodos, G., *AIChE J.* **16,** 300 (1970).
15. Reid, R. C., Prausnitz, J. M., and Sherwood, T. K., "The Properties of Gases and Liquids," 3rd ed. McGraw–Hill, New York, 1977.
16. Savage, W., M.S. thesis. University of California, Santa Barbara, 1982.
17. Chao, K. C., and Seader, J. D., *AIChE J.* **7,** 598 (1961).